Sensors and Materials, Vol. 12, No. 2 (2000) 99–108
MYU Tokyo

S & M 0400

Mechanical Characterization of Electroplated Nickel-Iron

Jan T. Ravnkilde[1], Volker Ziebart[2], Ole Hansen[1] and Henry Baltes[2]

[1]Mikroelektronik Centret, Technical University of Denmark
Bldg. 345 East, DK-2800 Lyngby, Denmark
[2]Physical Electronics Laboratory, ETH, CH-8093 Zurich, Switzerland

(Received January 24, 2000; accepted April 6, 2000)

Key words: electroplating, nickel-iron, mechanical properties, seed layer requirements

In this paper we present results of the mechanical characterization of electroplated nickel-iron (permalloy). The investigated plating bath is commonly used for MEMS applications, but no detailed mechanical characterization has been performed before. The following properties were investigated: residual stress, plane strain modulus, coefficient of linear thermal expansion (CTE) and mass density. The residual stress and plane strain modulus were derived from load-deflection measurements on long rectangular membranes. The CTE was extracted using the wafer curvature method. To obtain homogeneously thick electroplated films, the influence of the seed layer thickness on the current density distribution was investigated theoretically.

1. Introduction

Electroplated magnetic materials are of great interest in many MEMS devices such as magnetic yokes in printing heads,[1] magnetic flux concentrators for magneto-transistors,[2] μ-relays[3,4] and electromagnetic actuators.[5,6] Most magnetic microsystems demonstrated thus far have not depended on the mechanical properties of the plated layers since no movable structures have been included. If, however, devices such as μ-relays are to be fabricated, detailed information about the mechanical properties is required.

The elastic coefficients of MEMS materials influence the static and dynamic behavior of mechanical transducers. Residual stresses can cause devices to curl or buckle and layers

Correspondence: Jan T. Ravnkilde, Mikroelektronik Centret, Technical University of Denmark, Bldg. 345 East, DK-2800 Lyngby, Denmark. E-mail: jtr@mic.dtu.dk, tel: +45 4525 5700, fax: +45 4588 7762

to crack or delaminate. An elegant approach to the extraction of these parameters is the load-deflection method.[7] In this method a membrane made of the material to be characterized is fabricated and subsequently loaded using hydrostatic pressure. From the linear and nonlinear deflection response the mechanical properties of the membrane material such as residual stress and Young's modulus are derived.

Thermal properties of materials influence device operation at elevated temperatures. The coefficient of linear thermal expansion is extracted using the wafer curvature method, in which the thermally induced stress in a thin film on substrates with different CTEs is measured.

Electroplating a magnetic material such as permalloy (80% Ni, 20% Fe) is relatively difficult in comparison with electroplating pure metals such as nickel. Typically, the application sets specific requirements for the magnetic and mechanical properties of the deposit, *e.g.*, high permeability and low residual stress. As the magnetic and mechanical properties and composition and thickness of the plated layer depend on plating parameters such as current density, stirring and temperature, care must be taken to control these parameters precisely.

2. Fabrication

Nickel-iron membranes for load-deflection measurements were fabricated by the following process sequence (Fig. 1). Double polished 4" <100> Si wafers 380 μm thick were coated with 1.1-μm-thick low-stress PECVD silicon nitride. On the front of the wafers a 30-nm-thick Ti adhesion layer and a 300-nm-thick Cu seed layer were sputtered. A 7-μm-thick photoresist layer (Hoechst AZ4562) was spun on top of the seed layer and

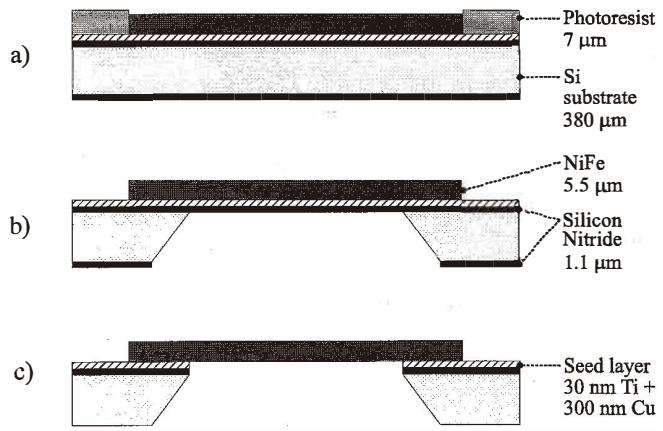

Fig. 1. Process sequence for the fabrication of nikel-iron membrance. a) Nickel-iron is electroplated in photoresist molds on top of a silicon-nitride coated wafer. b) Membranes are formed by anistropic etching of the Si wafer. c) Finally, the etch mask and seed layer are removed.

patterned to form electroplating molds for the membranes. Nickel-iron alloy was plated in the molds preceded by an activation of the seed layer in a fluorine-based acid (Fig. 1(a)). After stripping of the photoresist, a new layer of AZ4562 was spun and patterned on the backside of the wafers. Long rectangular windows were etched in the back surface silicon nitride using a SF_6 plasma, and subsequently the silicon was anisotropically etched in KOH (Fig. 1(b)). During etching the front surface of the wafers was protected. Finally, the front surface silicon nitride and the seed layer were removed (Fig. 1(c)).

Electroplating of nickel-iron was performed at room temperature using the bath formulation given in Table 1. The bath is known to give alloy deposits of approximately 80% Ni and 20% Fe.[8] It has been studied extensively because of its capability of producing soft magnetic films.[2,3,9] The wafer was mounted on a holder, which ensured electrical contact to the seed layer around the entire edge of the wafer. A separate cathode surrounded the wafer to "catch" stray current and thus improved the macroscopic material distribution across the wafer. A schematic of the electrode configuration is shown in Fig. 2. Two separate cathodes are required to control the amount of charge supplied to the wafer. Each membrane was surrounded by a 1-mm-wide nickel-iron ring to improve the material distribution across the membrane. In this way the variation in thickness of each membrane

Table 1.
Composition of nickel-iron electroplating bath. The bath is known to give alloys of approximately 80% Ni and 20% Fe.[8]

Nickel sulphate, $NiSO_4 \cdot 7H_2O$	200 g/l
Iron sulphate, $FeSO_4 \cdot 6H_2O$	8 g/l
Nickle chloride, $NiCl_2 \cdot 6H_2O$	5 g/l
Boric acid, H_3BO_3	25 g/l
Saccharin	3 g/l

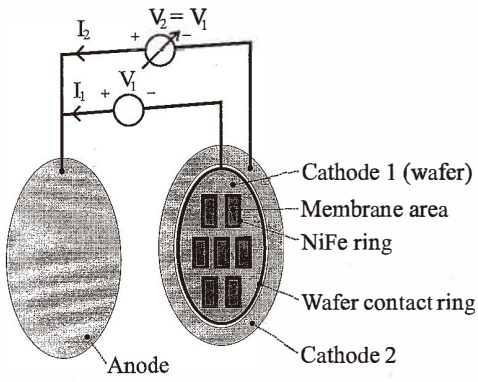

Fig. 2. Schematic showing the electrode configuration. A seperate cathode (Cathode 2) surrrounds the wafer to "catch" stray current.

was below 2%. A pure nickel foil with the same area as the two cathodes was used as the anode. To avoid depletion of iron ions, a fresh bath 3.5 l in volume was mixed when the iron concentration had changed by 0.1%.

The most important plating parameters in this type of bath are the current density and the amount of stirring. Their influence on the mechanical properties and the composition of the deposit was investigated for current densities in the range of 5 to 10 mA/cm^2 and for different levels of mechanical stirring using a propeller.

3. Results and Discussion

3.1 *Characterization of nickel-iron membranes*

The membranes were characterized using a setup that allows loading them with a differential pressure. The pressure was controlled to an accuracy of ±40 Pa using a pneumatic pressure controller DPI 520 from Druck Ltd. Deflection profiles and center deflections were determined using an optical profilometer from UBM with a Microfocus measurement head. This autofocusing instrument achieves a horizontal resolution of 1 μm and a vertical resolution of ±10 nm. Figure 3 shows a schematic of the measurement setup. For each stabilized pressure level a deflection profile was recorded by scanning the measurement head across the width a of the membrane. From each scan the center deflection w_0 was extracted. The precise width a and thickness h of each membrane was also measured using the optical profilometer. Figure 4 shows the measured center deflection w_0 as a function of the applied differential pressure p. The plain strain modulus $E/(1-\nu^2)$ and residual stress σ_0 were extracted from the experimental data using the load deflection model

$$p = C_1(\sigma_0, \frac{E}{1-\nu^2}, a, h)\ w_0 + C_3(\sigma_0, \frac{E}{1-\nu^2}, a, h)\ w_0^3, \tag{1}$$

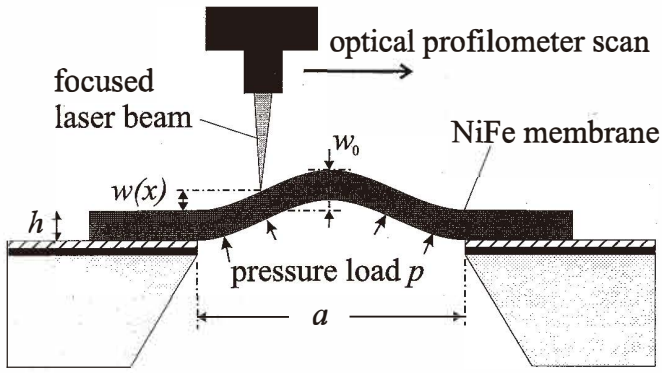

Fig. 3. Schematic of load-deflection measurment setup. The nickel-iron membrane is loaded with a differential pressure p. The center deflection w_0 is found by scanning across the width a of the membrane using an optical profilometer.

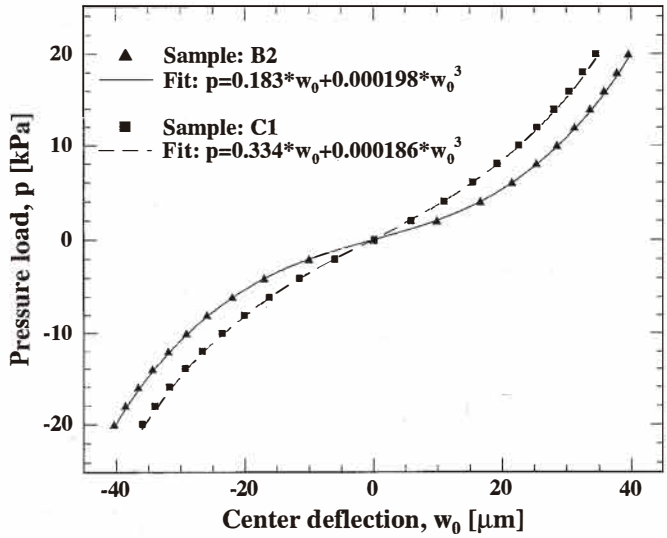

Fig. 4. Measured load-deflection curves (samples B2 and C1). Solid lines are fits using a cubic approximation.

which takes into account the flexural rigidity of the membranes.[10] The measurement setup and theory are described in detail in ref. (10).

The composition of the electroplated nickel-iron was measured directly on the fabricated membranes by quantitative energy dispersive spectrometry (EDS) using an X-ray detector from Rontec GmbH. These measurements were performed with an estimated absolute accuracy of ±2%.

Table 2 lists the plating parameters, the measured mechanical properties, and the membrane compositions. Current efficiencies*1 (C. E.) up to 88% were observed, where the highest C. E. was found for high current density and low stirring level. The results show that the plane strain modulus is independent of the current density and the amount of stirring in the ranges of interest. The average value of 135 GPa corresponds very well with previously reported values of Young's modulus (119 GPa) measured on 50/50 NiFe by tensile testing.[11] An assumed value of 0.28 of Poisson's ratio was used for the comparison. The residual stresses are low (25–71 MPa) and the variation can be explained by different stirring conditions, under which increased local disturbance of the catholyte layer causes an increased stress level in the deposit.[12] The measured compositions show the well-known anomalous codeposition effect of nickel-iron, where a preferential deposition of iron occurs. This results in an increased amount of iron in the deposit for low current densities or increased stirring.[13] With the plating parameters chosen here, however, we were not able to reach the desired 80% nickel and 20% iron. Improved control of the stirring by moving the sample or electrolyte in a controlled manner could give the desired

*1Defined as the relation between the actual and theoretical amounts of deposited material expressed in percent.

Table 2
Membrane dimensions (side length a, thickness h), plating parameters (current density j, stirring rate and current efficienty C.E.), mechanical properties stress σ_0, plane strain modulus $E/(1-\nu^2)$) and composition of mesured membranes.

Sample	Geometry		Plating parameters			Mechanical properties		Composition	
	a	h	j	stirring	C.E.	σ_0	$\frac{E}{1-\nu^2}$	Fe	Ni
	[μm]	[μm]	[mA/cm^2]	[rpm]	%	[MPa]	[GPa]	%	%
A1	3034	5.29	5.6	130	69	63	139	16.7	83.3
A2	3034	5.73	6.1	130	69	25	138	12.1	87.9
A3	2528	5.44	5.8	130	69	65	132	16.4	83.6
B1	3063	5.53	9.1	130	88	38	135	10.9	89.1
B2	3047	5.76	9.5	130	88	32	135	10.2	89.8
B3	2560	5.33	8.8	130	88	51	142	10.8	89.1
C1	3029	5.42	10.5	160	75	64	132	14.8	85.2
C2	2522	5.37	10.4	160	75	71	129	13.5	86.5

permalloy composition. Oxidation of Fe^{2+} to Fe^{3+} or depletion of iron during use of the bath also results in a lower iron content than expected. It is unlikely, however, that an alloy composition of 80% Ni and 20% Fe will change the plane strain modulus significantly.

3.2 *Wafer curvature measurements*

The coefficient of linear thermal expansion (CTE) of electroplated nickel-iron was determined by the wafer curvature method using a Tencor FLX-2320 thin-film stress measurement system. By monitoring the wafer curvature during heating cycles the temperature dependent residual stress of the plated layer was measured. Figure 5 shows typical cycles measured on Si and Cu substrates. The hysteresis of the first temperature cycle on the Si substrates is most likely caused by a relaxation of the sputtered Cu seed layer, as a similar effect was observed for measurements on Cu seed layers without plated nickel-iron. Copper was chosen as substrate material because of its high CTE in comparison with silicon. Temperature derivatives of the stress were –2.50 MPa/°C for Si substrates and 1.07 MPa/°C for Cu substrates. Cycles with a maximum temperature of 110°C and 210°C gave the same values within the accuracy of the setup. This results in a CTE of the NiFe α_{NiFe} (at room temperature) given by ref. (14)

$$\alpha_{NiFe} = \frac{\alpha_{Cu}\frac{d\sigma_{Si}}{dT} - \alpha_{Si}\frac{d\sigma_{Cu}}{dT}}{\frac{d\sigma_{Si}}{dT} - \frac{d\sigma_{Cu}}{dT}} = 12.3\times10^{-6}\,K^{-1} \qquad (2)$$

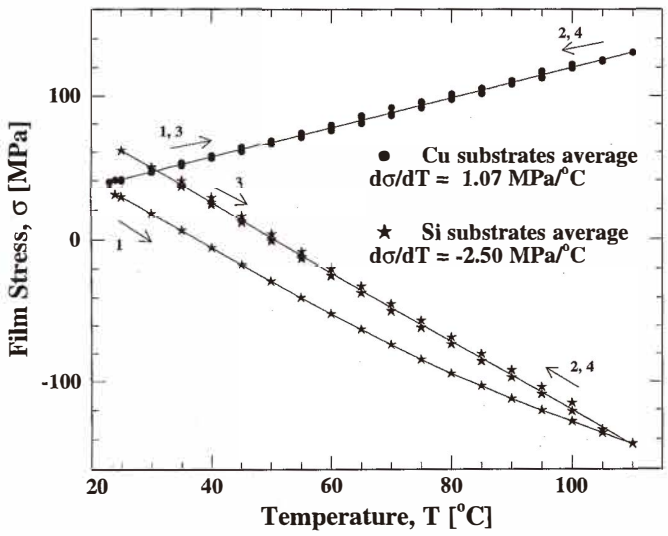

Fig. 5. Stress-temperature dependence of NiFe films on Si and Cu substrates. Two temperature cycles from room temperature to 110°C are shown for each substrate type.

where room temperature values for $\alpha_{Cu} = 16.5 \times 10^{-6}$ K^{-1} and $\alpha_{Si} = 2.6 \times 10^{-6}$ K^{-1} were used.[15]

By measuring the precise thickness of the plated nickel-iron at 107 points across the wafer, a mass density of 7.9 g/cm^3 was calculated from the thickness distribution, plated area and plated mass. The thickness of the plated nickel-iron was measured by scanning an optical profilometer across mesas fabricated by patterning and etching of the nickel-iron film.

4. Seed Layer Thickness

Several factors can cause a nonuniform current distribution, which in turn causes poor material distribution, nonuniform composition and internal stress. The most important factor is the geometry of the cathode. It is well known that the current density is higher in areas with protrusions and low structure density compared with areas with cavities and high structure density. Placement of dummy structures in areas with few isolated structures can improve the uniformity significantly. Another factor that is often neglected is the voltage drop in the seed layer from the contacts to the location of deposition. The seed layer voltage drop is particularly important to consider in baths without any levelling effect of the film growth.

The influence of the seed layer thickness h_s on the current distribution $j_z(r)$ was investigated theoretically using two assumptions: contact with the seed layer is made all around the edge of the wafer, and the catholyte has a conductance per area given by j/η,

where j is the average plating current density and η is the overvoltage[*2] at the cathode. The value of $j_z(r)$ is the initial current distribution at the beginning of a plating process. The final material distribution depends on the type of plating bath used, *e.g.*, the metal growth mechanism. Figure 6 shows a cross-section of the seed and catholyte layer drawn in cylindrical coordinates. By combining equations for the currents flowing through a seed layer section and the voltage drop across the catholyte and seed layer, we obtained Bessel's modified differential equation for the radial dependence of the plating current density j_z

$$r^2 \cdot \frac{d^2}{dr^2} j_z + r \cdot \frac{d}{dr} j_z - r^2 \frac{\rho_s j}{h_s \eta} j_z = 0, \tag{3}$$

where h_s and ρ_s are the thickness and resistivity of the seed layer, respectively. The solution to eq. (3) is given by

$$j_z(r) = j_z(0) I_0\left(\sqrt{\frac{\rho_s j}{h_s \eta}} r\right) \cong j_z(0)\left(1 + \frac{\rho_s j}{4 h_s \eta} r^2\right), \tag{4}$$

where $I_s(x)$ is the modified Bessel function ($n = 0$). The relative variation in thickness from the edge to the center of the wafer is defined by

$$\xi \triangleq \frac{j_z(R)}{j_z(0)} - 1, \tag{5}$$

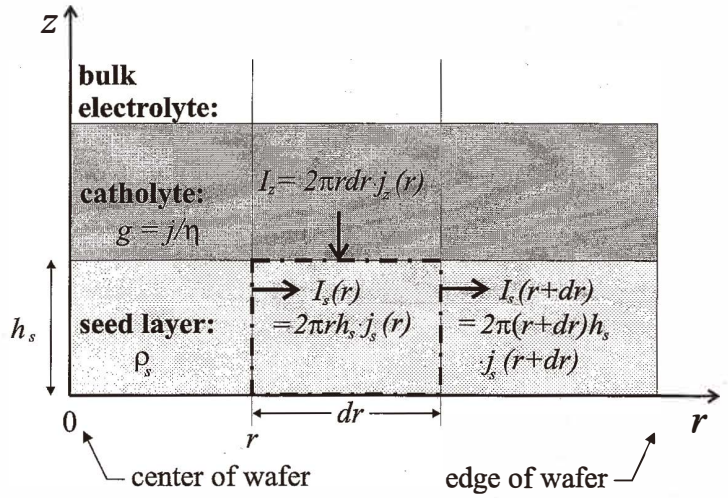

Fig. 6. Cross-section of seed and catholyte layer drawn in cylindrical coordinates. The currents flowing through a seed layer section are shown.

[*2]Defined as the difference between the potential at deposition and the potential at equilibrium.

where R is the radius of the wafer. By combining eqs. (4) and (5) the expression for the required thickness of the seed layer was obtained

$$h_s \geq \frac{\rho_s j R^2}{4\xi\eta}. \tag{6}$$

An example: A thickness variation less than 1% of the plated layer is required. Electroplating is performed with the plating parameters $j = 20$ mA/cm^2 and $\eta = 1$ V on 4" wafers using a copper seed layer. Using eq. (6) we can calculate the minimum required seed layer thickness to 250 nm. For less ideal distribution of contacts to the wafer such as a few point contacts, the requirement for the thickness of the seed layer is even larger. The simple model derived here only takes into account what happens at the beginning of a plating process when no material has been deposited on the seed layer. In a bath with no levelling effect the initial material distribution is continued throughout the plating process.

5. Conclusions

Mechanical properties of electroplated nickel-iron were characterized by load-deflection measurements on membranes and wafer curvature measurements. A plane strain modulus of 135 GPa, residual stresses in the range 25–71 MPa, CTE at room temperature of 12.3×10^{-6} K^{-1} and a mass density of 7.9 g/cm^3 were measured. Furthermore, a simple expression for the required thickness of the seed layer was derived.

Acknowledgments

The authors thank M. G. Allen, Georgia Institute of Technology, USA, and P. T. Tang, Technical University of Denmark for inspiring discussions. We also thank F. E. Rasmussen and C. B. Nielsen, Mikroelektronik Centret, for the EDS measurements.

References

1 F. Cardot, J. Gobet, M. Bogdanski and F. Rudolf: Sensors and Actuators A **43** (1994) 11.
2 M. Schneider, R. Castagnetti, M. G. Allen and H. Baltes: Proc. MEMS'95 (IEEE, Amsterdam, 1995) p. 151.
3 P. W. Taylor, O. Brand and M. G. Allen: J. MEMS **7** (1998) 181.
4 H. A. C. Tilmans, E. Fullin, H. Zied, M. D. J. Van de Peer, J. Kesters, E. Van Geffen, J. Bergqvist, M. Pantus, E. Beyne, K. Baert and F. Naso: Proc. MEMS'99 (IEEE Orlando, 1999) p. 25.
5 H. Guckel, T. R. Christenson, T. Earles, J. Klein, J. D. Zook, T. Ohnstein and M. Karnowski: Solid-State Sensor and Actuator Workshop (IEEE Hilton Head Island, South Carolina, 1994) p. 49.
6 C. Liu: Mechatronics **8** (1998) 613.
7 J. J. Vlassak and W. D. Nix: J. Materials Research **7** (1992) 3242.
8 M. Henstock and E. Spencer-Timms: Trans. Inst. Metal Finishing **40** (1963) 179.
9 J.-M. Quemper, S. Nicolas, J. P. Gilles, J. P. Grandchamp, A. Bosseboeuf, T. Bourouina and E. Dufour-Gergam: Sensors and Actuators A **74** (1999) 1.

10 V. Ziebart, O. Paul, U. Münch, J. Schwizer and H. Baltes: J. MEMS **7** (1998) 320.
11 E. Mazza, S. Abel and J. Dual: Microsystem Technologies **2** (1996) 197.
12 P. T. Tang: Department of Manufacturing Engineering, Technical University of Denmark, building 204, 2800 Lyngby, Denmark: Preliminary experiments show that increasing levels of stirring of this type of NiFe bath result in increasing levels of stress in the deposited NiFe layer.
13 P. Moller: Overflade Teknologi (Teknisk Forlag, Copenhagen, 1998) p. 123.
14 M. Maeda and K. Ikeda: J. Appl. Phys. **83** (1998) 3865.
15 Y. S. Touloukian, R. K. Kirby, R. E. Taylor and P. D. Desai: Thermophysical Properties of Matter (IFI / Plenum, New York, 1975) Vol. 12 p. 77, Vol. 13 p. 154.

Jan Tue Ravnkilde received his M.Sc. in electrical engineering from the Technical University of Denmark in 1997 and is curently working towards his Ph.D. degree. Mr. Ravnkilde is developing electroplated micro-electromechanical systems for fabrication on preprocessed integrated circuits.

Volker Ziebart received a diploma degree in physics from the University of Cologne in 1996 and a Ph.D. degree in physics from the Swiss Federal Institute of Technology, Zurich, in 2000. His thesis work focused on the mechanical and thermomechanical characterization of IC materials used for the fabrication of integrated micro-electromechanical systems (iMEMS). In 2000, he joined Phonak AG, Switzerland, where he is now working in the field of electronic packaging.

Ole Hansen received his M.Sc. in electronics from the Semiconductor Laboratory, the Technical University of Denmark, in 1977. Since 1977 he has been conducting research first at the Semiconductor Laboratory, the Technical University of Denmark, and then at the Microelectronics Centre (MIC), the Technical University of Denmark, in the fields of bipolar technology, CMOS technology, micromachining of Silicon, microsystems technology, microdevices by metal plating, scanning probe technology and biochemistry in microsystems. Since 1994 he has been an Associate Professor at MIC. He is presently teaching two lecture courses: Semiconductor Technology and Semiconductor Devices.

Henry Baltes received a D.Sc. degree from ETH Zurich in 1971. From 1974 to 1982 he worked for Landis & Gyr (now Siemens), Switzerland, where he directed the Solid-State Device Laboratory. From 1983 to 1988, he held the Henry Marshall Tory Chair at the University of Alberta, Edmonton, Canada, where he was also the acting President of the Alberta Microelectronic Centre and a cofounder and Director of the LSI Logic Corporation of Canada. Since 1988 he has been a Professor of Physical Electronics at ETH Zurich and directs the Physical Electronics Laboratory which is active in integrated micro-and nanosystems including electronic noses. From 1992 to 1996 he was the Program Director of the Swiss Federal Priority Program LESIT. In 1996, he was a Visiting Professor at Stanford University and the University of Waterloo. From 1996 to 1998 he served as Chairman of the Institute of Quantum Electronics of ETHZ. In 1998 he received the Koerber Award and in 1999 the Wilhelm-Exner Medal. He is a cofounder of ETH's spin-off company SENSIRION produces CMOS-based gas flow, humidity, and differential pressure sensors. Professor Baltes is a member of the Swiss Academy of Technical Sciences, a coeditor of Sensors Update, and a member of the technical program committees of MEMS and ESSDERC.